

# DESIGN AND EVALUATION OF AN EMTDC MODEL OF A CIRCULATING CURRENT DIFFERENTIAL PROTECTION TEST SYSTEM

C Wang P A Crossley H Y Li  
UMIST  
Manchester, UK

A D Parker  
GEC ALSTHOM T&D  
Stafford, UK

*Keywords: current transformer, EMTDC, simulation, differential current protection.*

## ABSTRACT

The proposed paper describes the design and evaluation of a simulator suitable for the type-testing of a circulating current differential protection relay. The simulator uses EMTDC to model the effect on the primary current signals of a fault on the primary power system. The primary current signals, measured at both ends of a feeder, are processed by an EMTDC model of the complete secondary protection system. The model includes current transformers, connecting leads, stabilising resistors and an impedance that represents the ac burden of the relay being tested. The output from this model is a data file that describes the secondary current signals seen by the relay if it was connected into the simulated protection system. To test an actual relay, the date file is transferred to a relay test set and replayed in real time via A-D converters and current amplifiers. To illustrate the validity of the simulator, the paper includes results that compare the simulated signals with those recorded on a high current Synthetic Test Plant. The Synthetic Test Plant has been used for more than 30 years in the type testing of differential protection systems.

## 1. INTRODUCTION

During the last few years several research papers have recognised the need for a more accurate CT model for use in the type testing of protection relays. Kezunovic carried out experimental evaluation of CT models implemented using the EMTP simulator [1]. O'Kelly used multiple valued B-H (or  $\lambda$ -I) characteristic of an iron core in his current transformer model [2]. Li used an ADSP21020 DSP card to implement a real time current transformer simulation based on the O'Kelly model [3]. J R Marti described a current transformer model with fast solution algorithms [4]. This fast and non-iterative solution method evaluated the secondary current from a CT under a known primary current condition.

In this paper the authors will show that the equations associated with a single CT model [4] can be extended to two CTs operating within a current differential protection scheme.

## 2. TWO CT ALGORITHM

### 2.1 The differential current protection scheme

A diagram describing the structure of a circulating current differential protection scheme is shown in Fig. 1.

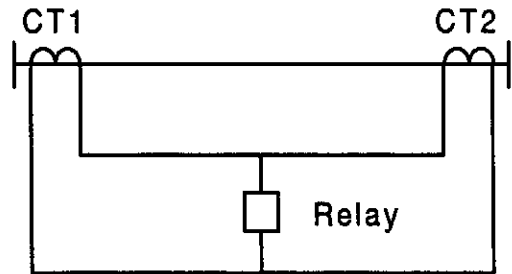


Fig. 1 Differential current protection scheme

### 2.2 The equivalent circuit of a two CT model

The electrical equivalent circuit can be represented as:-

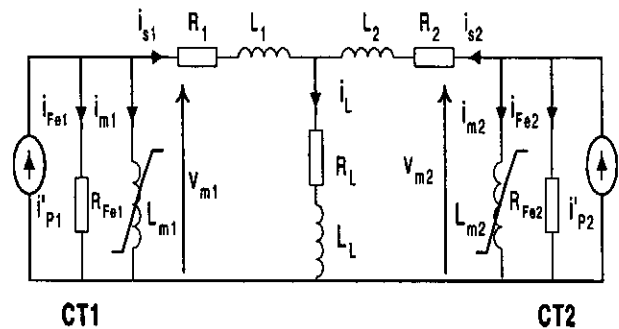


Fig. 2 Equivalent circuit

where:

- $i'_{p1}$ ,  $i'_{p2}$  are the CT1 and CT2 primary currents referred to the secondary.
- $i'_{Fe1}$ ,  $i'_{Fe2}$  are the currents through the resistances  $R_{Fe1}$  &  $R_{Fe2}$ , that represent the iron core losses.
- $i_{m1}$ ,  $i_{m2}$  are the magnetising currents through the non-linear inductances  $L_{m1}$  &  $L_{m2}$ , that represent the magnetising behaviour of the iron core.
- $v_{m1}$ ,  $v_{m2}$  are the voltages across the magnetising branches.
- $i_{s1}$ ,  $i_{s2}$  are the secondary currents.
- $i_l$  is the current through the operating coil of the relay.

### 2.3 Core loss branches

For CT1:- 
$$v_{m1} = R_{Fe1} i'_{Fe1} = \frac{d}{dt} \lambda_1$$

$$\therefore \frac{1}{\Delta t} (\lambda_{1,new} - \lambda_{1,old}) = \frac{1}{2} R_{fe1} (i'_{Fe1,new} + i'_{Fe1,old})$$

i.e. 
$$i'_{Fe1,new} = C_{Fe1} \lambda_{1,new} + h_{Fe1,old}$$

where:- 
$$h_{Fe1,old} = - C_{Fe1} \lambda_{1,old} - i'_{Fe1,old}$$

$$\text{and } C_{Fe1} = \frac{2}{R_{Fe1}\Delta t}$$

Similarly, the current in the  $R_{Fe2}$  term of CT2 is:-

$$i_{Fe2.new} = C_{Fe2}\lambda_{2.new} + h_{Fe2.old}$$

where:-  $h_{Fe2.old} = -C_{Fe2}\lambda_{2.old} - i_{Fe2.old}$

$$\text{and } C_{Fe2} = \frac{2}{R_{Fe2}\Delta t}$$

## 2.4 Magnetising branches

For the magnetising branch in CT1:-

$$i_{m1.new} - i_{m1.old} = \frac{1}{L_{m1}} (\lambda_{1.new} - \lambda_{1.old})$$

The magnetising current in CT1 is:-

$$i_{m1.new} = \frac{1}{L_{m1}} \lambda_{1.new} + k_{m1}$$

where:-  $k_{m1} = i_{m1.old} - \frac{1}{L_{m1}} \lambda_{1.old}$

Similarly, the magnetising current in CT2 is:-

$$i_{m2.new} = \frac{1}{L_{m2}} \lambda_{2.new} + k_{m2}$$

where:-  $k_{m2} = i_{m2.old} - \frac{1}{L_{m2}} \lambda_{2.old}$

$L_{m1}$  &  $L_{m2}$  are the slopes of the CT1 & CT2  $\lambda$ - $I_m$  curves:

$$L_{m1} = \frac{1}{\frac{df_1(\lambda)}{d\lambda}} = \frac{1}{f_1'(\lambda)} \quad \text{and} \quad L_{m2} = \frac{1}{\frac{df_2(\lambda)}{d\lambda}} = \frac{1}{f_2'(\lambda)}$$

where  $i_{m1} = f_1(\lambda)$  and  $i_{m2} = f_2(\lambda)$  are obtained from  $H=g_1(B)$  and  $H=g_2(B)$  which represents a given B-H characteristic of a real CT, as shown in Fig. 3.

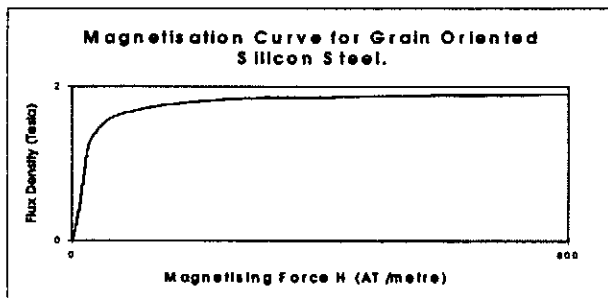


Fig. 3 B-H curve

## 2.5 Secondary side branches

According to the equivalent circuit:-

$$v_{m1} = R_1 i_{S1} + L_1 \frac{d(i_{S1})}{dt} + R_L (i_{S1} + i_{S2}) + L_L \frac{d(i_{S1} + i_{S2})}{dt}$$

$$\begin{aligned} &= (R_1 + R_L) i_{S1} + (L_1 + L_L) \frac{d(i_{S1})}{dt} + R_L i_{S2} + L_L \frac{d(i_{S2})}{dt} \\ &= R_1' i_{S1} + L_1' \frac{d(i_{S1})}{dt} + R_L i_{S2} + L_L \frac{d(i_{S2})}{dt} \end{aligned}$$

where:-  $R_1' = R_1 + R_L$ ;  $L_1' = L_1 + L_L$

$$v_{m1} = \frac{d}{dt} \lambda_1 = \frac{1}{\Delta t} (\lambda_{1.new} - \lambda_{1.old})$$

$$\begin{aligned} &= \frac{1}{2} R_1' (i_{S1.new} + i_{S1.old}) + \frac{1}{\Delta t} L_1' (i_{S1.new} - i_{S1.old}) \\ &\quad + \frac{1}{2} R_L (i_{S2.new} + i_{S2.old}) + \frac{1}{\Delta t} L_L (i_{S2.new} - i_{S2.old}) \end{aligned}$$

Hence:-

$$\begin{aligned} \lambda_{1.new} &= \lambda_{1.old} + \frac{1}{2} R_1' \Delta t (i_{S1.new} + i_{S1.old}) + L_1' (i_{S1.new} - i_{S1.old}) \\ &\quad + \frac{1}{2} R_L \Delta t (i_{S2.new} + i_{S2.old}) + L_L (i_{S2.new} - i_{S2.old}) \\ &= \lambda_{1.old} + \left(\frac{1}{2} R_1' \Delta t + L_1'\right) i_{S1.new} + \left(\frac{1}{2} R_1' \Delta t - L_1'\right) i_{S1.old} \\ &\quad + \left(\frac{1}{2} R_L \Delta t + L_L\right) i_{S2.new} + \left(\frac{1}{2} R_L \Delta t - L_L\right) i_{S2.old} \end{aligned}$$

$$\lambda_{1.new} = A_{11} i_{S1.new} + A_{12} i_{S2.new} + A_{13} \quad (1)$$

where

$$A_{11} = \frac{R_1' \Delta t}{2} + L_1' \quad A_{12} = \frac{R_L \Delta t}{2} + L_L$$

$$A_{13} = \lambda_{1.old} + \left(\frac{R_1' \Delta t}{2} - L_1'\right) i_{S1.old} + \left(\frac{R_L \Delta t}{2} - L_L\right) i_{S2.old}$$

Similarly, the flux in CT2 is:-

$$\lambda_{2.new} = A_{21} i_{S1.new} + A_{22} i_{S2.new} + A_{23} \quad (2)$$

where

$$A_{22} = \frac{R_2' \Delta t}{2} + L_2' \quad A_{21} = \frac{R_L \Delta t}{2} + L_L$$

$$A_{23} = \lambda_{2.old} + \left(\frac{R_2' \Delta t}{2} - L_2'\right) i_{S2.old} + \left(\frac{R_L \Delta t}{2} - L_L\right) i_{S1.old}$$

and

$$R_2' = R_2 + R_L; \quad L_2' = L_2 + L_L$$

The primary current in CT1 referred to the secondary is:-

$$\begin{aligned} i_{p1.new} &= i_{Fe1.new} + i_{m1.new} + i_{S1.new} \\ &= C_{Fe1} \lambda_{1.new} + h_{Fe1.old} + \frac{1}{L_{m1}} \lambda_{1.new} + k_{m1} + i_{S1.new} \\ &= \left(C_{Fe1} + \frac{1}{L_{m1}}\right) \lambda_{1.new} + i_{S1.new} + (h_{Fe1.old} + k_{m1}) \end{aligned}$$

Therefore:-

$$i_{S1.new} = -\left(C_{Fe1} + \frac{1}{L_{m1}}\right) \lambda_{1.new} - (h_{Fe1.old} + k_{m1} + i_{p1.new})$$

$$\text{i.e. } i_{S1.new} = B_{11} \lambda_{1.new} + B_{12} \quad (3)$$

where:  $B_{11} = -\left(C_{Fe1} + \frac{1}{L_{m1}}\right)$ ,  $B_{12} = -(h_{Fe1.old} + k_{m1} + i_{p1.new})$

$$\text{Similarly:- } i_{S2.new} = B_{21} \lambda_{2.new} + B_{22} \quad (4)$$

where:-  $B_{21} = -(C_{Fe2} + \frac{1}{L_{m2}})$ ,  $B_{22} = -(h_{Fe2,old} + k_{m2} \cdot i_{p2,new})$

## 2.6 Calculation of $i_{S1,new}$ , $i_{S2,new}$ , $\lambda_{1,new}$ , $\lambda_{2,new}$

The four variables  $i_{S1,new}$ ,  $i_{S2,new}$ ,  $\lambda_{1,new}$  and  $\lambda_{2,new}$  can be calculated from equations (1)-(4). Furthermore, the other variables  $i_{m1,new}$ ,  $i_{m2,new}$ ,  $i_{L,new}$ ,  $V_{m1,new}$ ,  $V_{m2,new}$ ,  $i_{Fe1,new}$  and  $i_{Fe2,new}$  can also be calculated.

## 3. IMPLEMENTING THE ALGORITHM IN EMTDC

The algorithm for the two CT differential protection scheme has been designed and constructed using the EMTDC simulator. The parameters and magnetising characteristic of each of the CTs and the burden can be adjusted separately. The outputs are the secondary current, the magnetising force and the flux density in each CT and the differential current in the relay.

## 4. COMPARISON BETWEEN RESULTS SIMULATOR & SYNTHETIC TEST PLANT

This section compares the results obtained from the simulator with those obtained from a synthetic test plant (STP). Three test cases are described all with the same initialisation condition, i.e. the remanence in the CTs, at the start of each test, are approximately equal. During initialisation, each CT was driven to the same heavily saturated state. This was necessary because of the difficulty in setting the remanent flux of a real CT in the synthetic test plant to zero.

For the test results, the CT burdens were assumed to be purely resistive and leakage inductances were neglected.

### 4.1 Case-1

The simulation results and the STP results for case-1 were obtained under the same test conditions, i.e.  $X/R=40$ ; external fault; point on wave  $270^\circ$ ;  $R_{ct1}=1.5\Omega$ ;  $R_{ct2}=6.5\Omega$  and  $R_L=3\Omega$ . The comparisons between the simulated and experimental CT1 secondary current, CT2 secondary current and the differential current are shown in Fig. 4 to 6 respectively.

Comparing Fig.4 with Fig.6, we observe that CT2 is more heavily saturated than CT1. This is because the lead resistance connecting CT2 to the relay is larger than that used with CT1 ( $R_{ct2}=6.5\Omega$  vs.  $R_{ct1}=1.5\Omega$ ). This difference results in a significant magnitude of differential current that flows through the relay.

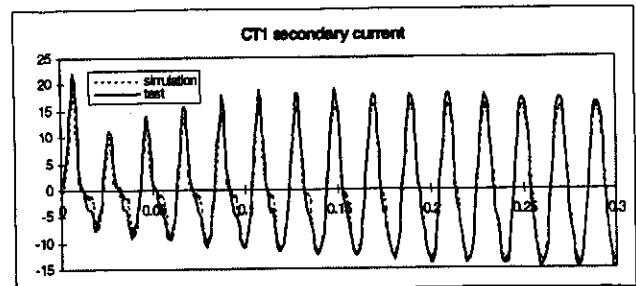


Fig. 4 Secondary current from CT1

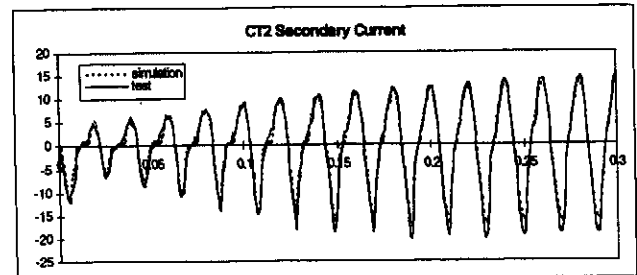


Fig. 5 Secondary current from CT2

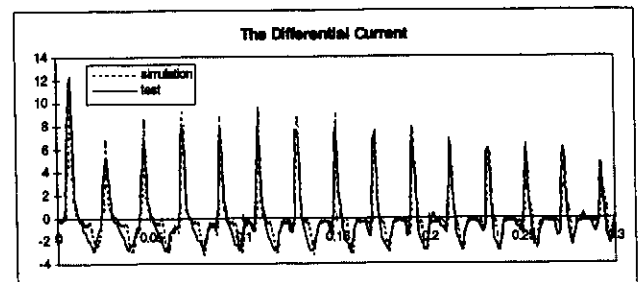


Fig. 6 Differential current

### 4.2 Case-2

The simulation results and the STP results for case-2 were obtained under the same test conditions, i.e.  $X/R=40$ ; external fault; point on wave  $270^\circ$ ;  $R_{ct1}=1.5\Omega$ ;  $R_{ct2}=1.5\Omega$  and  $R_L=3\Omega$ . The comparisons between the simulated and experimental CT1 secondary current, CT2 secondary current and the differential current are shown in Fig. 7 to 9 respectively.

The only difference between case-2 and case-1 is the reduction in the lead resistance for CT2 from  $6.5\Omega$  to  $1.5\Omega$ . Since, there is now no imbalance between the resistances of the leads used to connect each CT to the relay, the level of saturation in the CTs are similar and the differential current is very small.

The only difference between case-2 and case-1 is the reduction in the lead resistance for CT2 from  $6.5\Omega$  to  $1.5\Omega$ . Since, there is now no imbalance between the resistances of the leads used to connect each CT to the relay, the level of saturation in the CTs are similar and the differential current is very small.

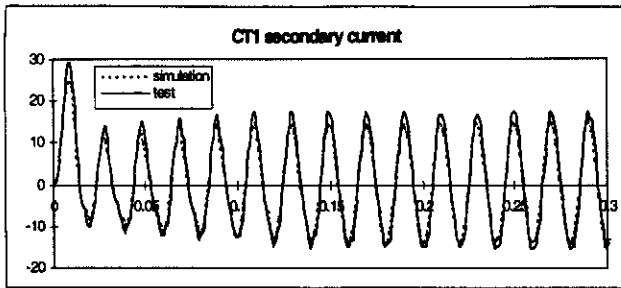


Fig. 7 Secondary current from CT1

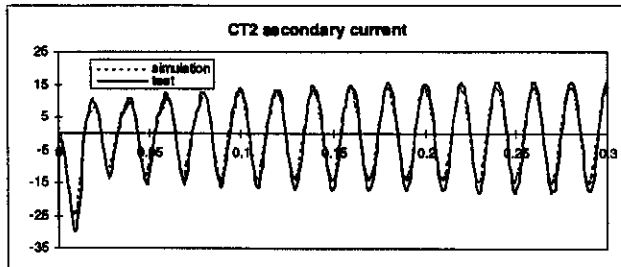


Fig. 8 Secondary current from CT2

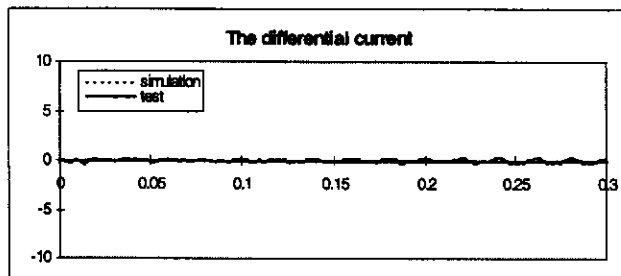


Fig. 9 Differential current

#### 4.3 Case-3

The simulation results and the STP results for case-3 were obtained under the same test conditions, i.e.  $N/R=40$ ; external fault; point on wave  $270^\circ$ ;  $R_{ct1}=1.5\Omega$ ;  $R_{ct2}=6.5\Omega$  and  $R_L=100\Omega$ . A comparison between the simulated and experimental CT1 secondary current, CT2 secondary current and the differential current are shown in Fig. 10 to 12 respectively.

The only difference between the test conditions in case-3 and case-1 is the large increase in the ohmic value of the stabilising resistor  $R_L$ . The effect of this resistor ensures that in case-3, the differences in the lead resistances does not result in a differential current of significant value.

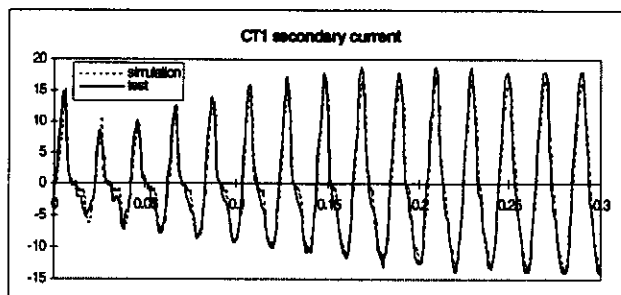


Fig. 10 Secondary current from CT1

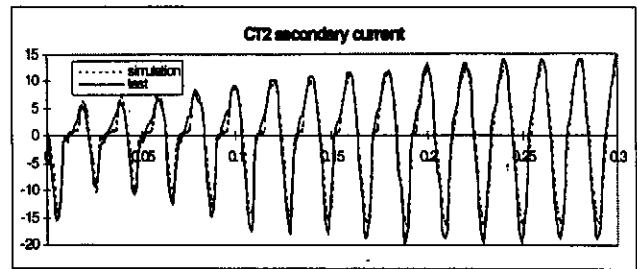


Fig. 11 Secondary current from CT2

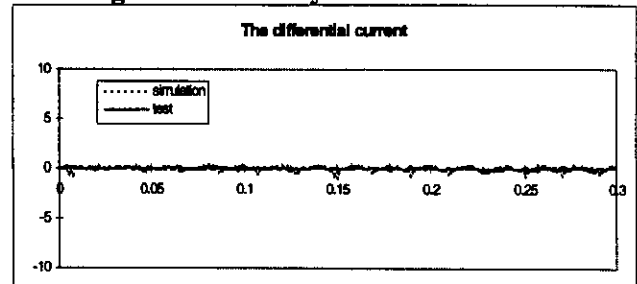


Fig. 12 Differential current

## 5. CONCLUSIONS

A circulating current differential protection test system has been designed and constructed using the EMTDC/PSCAD simulator. The results from the simulator are very similar to those obtained on a synthetic test plant used by a manufacturer for over 30 years to type test circulating current differential protection schemes. The simulator has the following features: it uses a fast and non-iterative algorithm; the B-H curve of each CT can be easily adjusted in accordance with material used in the CT core; and the parameters and magnetising characteristic of each CT and the burden can be adjusted separately.

Data generated by the EMTDC simulator can be replayed by a relay test set and injected into an actual differential relay. The input signals seen by the relay are almost identical to those it would see if it was being tested on a synthetic test plant.

## REFERENCES

- [1] M Kezunovic, et. al, "Experimental Evaluation of EMTDC-based Current Transformer Models For Protective Relay Transient Study", IEEE Transactions on Power Delivery, Vol. 9 No.1, January 1994.
- [2] O'Kelly, et. al, "Simulation of Transient and Steady-state Magnetisation Characteristics with Hysteresis", IEE Proc. Vol. 124, No.6, June 1977.
- [3] H Li, P A Crossley and M Uang, "The Use of Digital Signal Processors For Real Time Digital Current Transformer simulation", Second International Conference on Digital Power System Simulators, Montreal, Quebec, Canada, May, 1997.
- [4] J R Martin, L R Linares and H W Dommel, "Current Transformer and Coupling-Capacitor Voltage Transformers in Real-time Simulation", IEEE 96 SM 389-7PWRD.